3D printing of gels based on xanthan/konjac gums

P. García-Segovia, V. García-Alcaraz, S. Balasch-Parisi, J. Martínez-Monzó

PII: S1466-8564(20)30289-7

DOI: https://doi.org/10.1016/j.ifset.2020.102343

Reference: INNFOO 102343

To appear in: *Innovative Food Science and Emerging Technologies*

Received date: 14 June 2019

Revised date: 7 January 2020

Accepted date: 18 March 2020

Please cite this article as: P. García-Segovia, V. García-Alcaraz, S. Balasch-Parisi, et al., 3D printing of gels based on xanthan/konjac gums, *Innovative Food Science and Emerging Technologies* (2020), https://doi.org/10.1016/j.ifset.2020.102343

3D printing of gels based on xanthan/konjac gums.

P. García-Segovia[a], V. García-Alcaraz[a], S. Balasch-Parisi[b], J. Martínez-Monzó[a*].

[a]*Food Technology Department, Universitat Politècnica de València, Camino de Vera s/n., 46022 Valencia, Spain.*

[b]*Departamento de Estadística e Investigación Operativa, Universitat Politècnica de València, Camino de Vera s/n., 46022 Valencia, Spain.*

*Corresponding author. Tel.: 00 34 963879364; fax: 00 34 963877369. E-mail address: xmartine@tal.upv.es (J. Martínez-Monzó)

ABSTRACT

3D printing technology is a promising technology with the possibility of use for developing personalised food. To make this technology easier, and readily available for consumers, greater knowledge of the printing conditions and characteristics of food-ink is needed. This paper investigates the printability of gels based on syrup, xanthan, and konjac gums, while affecting printing variables. Those variables include the printing temperature (25 ºC and 50 ºC) and the composition of the product analysed using rheological and textural characterisation techniques. Also, the link between rheological and textural properties of gels, and printability was analysed. The higher values of G', G" and η* correlated to the mixtures with lower syrup concentration, and higher values of xanthan and konjac gum. Syrup, xanthan gum and konjac gum content influenced the textural properties. With the increase of syrup content, the Fmax, Fmean, Area, and slope showed reductions giving more weak gels. Rheological and textural values can define composition of formulations that give rise to valid 3D printed figures.

Industrial relevance

There is an increasing market need for customized food products. Three-dimensional (3D) food printing will be developed in the coming years. Undoubtedly, food printing can have many advantages, but whether the market is ready for such a big change and the technology will grow fast enough are the questions. Also it seems to be the right solution to meet the needs of today's consumers who increasingly have too little time to prepare meals on their own, especially in small or single-person households. In the future, ready, healthy meal, tailored to their individual needs, will be waiting when coming home. 3D printed gels can contribute to develop personalized food with specific nutritional characteristics. For example, this kind of gels can be used to manufacture soft foods for the elderly who have problems to swallow.

Key words: 3D printing, rheological properties, extrusion, konjac gum, xanthan gum

1. Introduction

Additive manufacturing (AM), referred to as 3D printing, has received a large amount of attention from industry, academia, and the public for its many advantages. AM offers shorter production time compared with traditional manufacturing methods. In addition, it can generate various complex shapes by using a limited mass of materials, with an enhancement of mechanical properties (Godoi, Prakash, & Bhandari, 2016; Wang, Zhang, Bhandari, & Yang, 2018). The potential advantages of 3D printing technology can be applied within the food sector, such as customised food design, personalised, and digitalised nutrition, simplifying supply chain, and expansion of source food material. Using this technology, some complex and fantastic food designs, which cannot be achieved by manual labour or conventional moulds, can be produced by ordinary people based on predetermined data files compromising culinary knowledge and artistic skills from chefs, nutrition experts, and food designers (Liu, Zhang, Bhandari, & Wang, 2017; Sun et al., 2015). The properties and composition of materials are considered the key factors for the 3D printing process. These materials should be homogeneous with appropriate flow properties, suitable for extrusion but able to support its structure during and after the printing process (Godoi et al., 2016; Fanli Yang, Zhang, Bhandari, & Liu, 2018). Zhang et al. (2015) used dual-responsive hydrogels to fabricate three-dimensional objects via extrusion from a nozzle in 3D printing. They found gels with a rapid and reversible modulus response to shear stress and temperature were suitable for direct-write 3D printing; they were easily extruded from nozzle tip during printing and could maintain sufficient mechanical integrity to support the next printed layer, without deformation (Zhang et al., 2015). Other researchers have come to similar conclusions (Wang et al., 2018). However, the correlation between the food material's rheological properties and 3D printing behaviour have not been widely investigated (Liu et al., 2017). Rheological properties of gels significantly affect the printability, therefore are important criteria to judge 3D printing materials (Liu et al., 2017; Fanli Yang et al., 2018). The effect of temperature on rheological properties can be a parameter to consider in 3D printing, meaning its control must be considered in the design of printers.

During the extrusion process, rheological properties of materials are critical for providing proper extrudability, binding of different foodstuff layers, and to support the weight of deposited layers. In food printing, soft materials, such as dough and meat pastes have been utilised to print 3D objects (Godoi et al., 2016). Apparent viscosity is an important factor which should be low enough to allow for easy extrusion but high enough to adhere to previous deposited layers (Liu, Zhang, Bhandari, & Yang, 2018). Until last year, limited information on the effects of the printer variables such as temperature of food, travel speed, print speed, infill levels, and layer height, on the printing performances of the food were available (Carla Severini & Derossi, 2016). 2018, however, has seen an increase in the number of investigations of rheological characteristics, and effect of printing conditions, on the properties of several printed food snacks, including, potato puree, lemon juice gel, surimi, vegetables, sauces and processed cheese (Derossi, Caporizzi, Azzollini, & Severini, 2018; Hamilton, Alici, & in het Panhuis, 2018; Holland, Foster, MacNaughtan, & Tuck, 2018; Le Tohic et al., 2018; C. Severini, Azzollini, Albenzio, & Derossi, 2018; Yang et al., 2018). These previous papers reveal the increasing interest in information of printing parameters and physicochemical properties of food, allowing improvement of food printers. 3D food printing is far more complex than it appears. There are several conditions that need optimising in 3D food printing, including proper application of mechanical force, careful design of the digital recipe, and suitable feeding ingredients. Different food formulations are necessary when different pressures are applied. Sometimes room temperature may also affect the food mixture flow rate through the food nozzle (Lipson & Kurman, 2013). While determining the food recipes, the properties of food materials should be considered; the materials should have high strength, to fit the needs of product printability (Fan Yang, Zhang, & Bhandari, 2017). Concurrently, the temperature of the food during the printing process may be a key factor considering rheological properties. At present, there is little work that analyses the effect of printing temperature on the characteristics of final product rheological properties of 3D printed food (Liu, Bhandari, Prakash, Mantihal, & Zhang, 2019; Dianez et al., 2019). The aim of this paper was to study the printability of gels

based on xanthan/konjac gums when affected by printing variables, such as, the printing temperature and rheological and textural properties, analysing the composition of the product.

2. Material and methods

2.1. Raw materials

Xanthan gum was kindly provided by Solé Graells S.A. (Barcelona, Spain). Glucomannan (KGM), Calcium lactate hydrate (CLH), and calcium gluconate anhydrous (CGA) were supplied by Sosa Ingredients S.L. (Moià, Spain). Sugar was purchased from a local supermarket. Colourant, Brilliant Blue E133, was supplied by ROHA EPSA S.L. (Torrent, Spain).

2.2. Preparation of solutions

The food-inks were formulated as water solutions composed of different concentrations of xanthan gum, KGM and sugar syrup (100 mL water, 20 g of sugar, 2g of CLH/CGA and 1 µg colourant). Table 1 summarises the levels of the food-ink constituents and operational parameters used in the experimental design. The Syrup was prepared with a sugar and CLH/CGA dispersion in distilled water at room temperature. After dispersion of syrup ingredients, a colourant was added to improve visualisation of food-ink. Solutions were prepared by hot dispersion of the polymers (xanthan gum and KGM) in the syrup, according quantities described in Table 1. Samples of food-ink were mixed using a magnetic stirrer, while heating to 90 ºC and held at that temperature for 20 min. After, the mixing process samples were cooled to 4 ºC and maintained in a refrigerated area at this temperature for 24 h prior to printing process. Before use in the 3D printer, food-inks were introduced in the syringe and tempered at an extrusion temperature (25 ºC or 50 ºC).

2.2. Rheological characterisation

Rheological oscillation testing, of the solutions and gels, was performed in using a rheometer (Kinexus pro+, Malvern instruments, Worcestershire, UK), controlled with commercial computer software (rSpace, Rheometry software for Kinexus). Samples were analysed using a

25 mm plate-plate geometry (DSR II, Upper Plate) with a 1 mm gap setting between the plates and a heat-controlled sample stage (Peltier Cylinder Cartridge, Malvern instruments, Worcestershire, UK). The upper plate was lowered onto the sample, following the Kinexus SOP, the excess sample, expelled from the geometry, was trimmed off. Samples were loaded with minimal disturbance at room temperature, to minimise the loss of water the periphery of the was sample coated with a light silicone oil, and left unperturbed for 5 min before measurements were made. A temperature sweep was conducted by heating at 2 ºC/min, with measurements made at a frequency of 1 Hz and a strain of 0.5%. This ensured that data obtained was in the linear viscoelastic region. Results are the average of three replicates (a new sample was loaded for each repetition).

2.3. Extrusion assay

Texture measurements for the food-inks was performed using a texture analyser (model TA-XT2, Stable Micro System Ltd., Leicestershire, UK), with the ‘‘Forward Extrusion Cell’’ attachment (HDP/FE). The syringe used in the printing process, a cylindrical chamber of 35 mm diameter and 100 mm height, with a piston of 35 mm diameter, was used in the extrusion assay. The chamber of the syringe was filled with food-ink to 80 mm, the piston was placed at 80 mm (in contact with the sample) and moved 10 mm. The sample was extruded through a 2 mm diameter hole. The parameters set were: pre-test speed, 0.075 mm/s; test speed, 0.075 mm/s; post-test speed, 2 mm/s; trigger force 5 g. The test speed was selected to simulate the extrusion speed in the printer (70 mm^3/s). The measurements were made at a controlled temperature (25 ºC and 50 ºC), using a cooling coil to cover the cylindrical measurement chamber while connected to a circulating water bath (Heildolph rotacool chiller, Heildolph, Illinois, USA). Temperatures of the samples were monitored during test. The measurement of the texture was performed in triplicate for each sample.

2.4. Printing process

This study used a commercial 3D printer (BCN 3D+, BCN3D Technologies, Barcelona, Spain) equipped with a paste extruder nozzle to work with food materials (Paste extruder, BCN3D Technologies, Barcelona, Spain). The 3D printing system composed of the following two major parts: an extrusion system (syringe) and an X-Y-Z positioning system using stepper motors. A five points star (inscribed in a square of 80 mm width by 20 mm height) with four external perimeters and a complete base was extruded at varying temperatures (Figure 1a). The figure was created with a free online commercial program (Thinkercad, Autodesk, Inc., San Rafael, California, USA). A computer with another free program (Slic3r, free software, developed by Alessandro Ranellucci with the help of contributors and community), to provide g-code files to the printer, controlled the motion and positioning. The printing process was conducted at different temperatures (25 ºC and 50 ºC) and as previously stated was controlled using a cooling coil (Figure 1b). The nozzle height was set at 2 mm from the printing bed and was achieved by adjusting the whole feeding device, each successive layer applied 1.5 mm. The pressure exerted on the sample was applied via the extruder piston. The samples were extruded onto a plastic polymer plate using nozzles of circular shape with a diameter of 2.0 mm. To assess the effects on the extruded geometry, line tests were used. Lines of sample were extruded at varying extrusion rates, at the same rates of movement, to determine the appropriate extrusion speed, these conditions were fixed to 15 mm/s for extrusion speed with a volumetric flow rate of approximately 70 mm^3/s for food-ink.

2.5. Image analysis

Pictures of each printed formulation were taken at 5 min and 1 hour after the printing process. Pictures were analysed using the software, Image J (http://rsb.info.nih.gov/ij/; (Abramoff, Magalhães, & Ram, 2004). Different dimensions were measured as shown Figure 2. In this study, area and height of the printed star were select as shape parameters. These parameters can be easily evaluated to analyse the dimensional changes of the figure with time.

2.6. Experimental design and statistical analysis

In this work, the Minitab 18 Statistical Software (Minitab Inc., USA) was used for mixture design and analysis of experimental data. Also, for optimisation of the required proportions of three-component mixtures (food-ink) of syrup (x_1), xanthan gum (x_2), KGM (x_3), and one process variable (z, temperature of printing), for the printing of a five points star. Mixtures were designed so all proportions of all substrates in each formulation were the sum of 100% for a mixture load of 100 g (Cornell, 1990), the weight percent ranges were: $97.7 \leq x_1 \leq 98.25$, $0.5 \leq x_2 \leq 0.65$, and $1.25 \leq x_3 \leq 1.65$. These ranges were selected from previous experiments. The Minitab software using axial mixture design (3q+1) generated 26 runs for two levels of the process variable (25 ºC and 50 ºC). For each formulation shape parameter, textural and rheological parameters were determined, experimentally, prior to modelling and optimisation of the mixture proportion by the software. The designed formulations of mixtures, and temperatures, defined by the software, for these investigations are given in Table 1. To evaluate the relationship of the responses on the three significant independent variables and process variables; a model that includes components of the mixture and their interactions and temperature of printing was used (equation 1). The regression equation for a mixture design is usually formulated as polynomial that has no constant term. The polynomial for a mixture design does not have any squared terms. Curvature is represented by interaction terms. The type of blending that we can analyse with the model used is a blend with additive effect of each variable, nonlinear synergistic binary effect of the components, and influence of one process variable.

$$E(y)=x_1(\beta_1+\alpha_1 z)+x_2(\beta_2+\alpha_2 z)+x_3(\beta_3+\alpha_3 z)+x_1x_2(\beta_{12}+\alpha_{12} z)+x_1x_3(\beta_{13}+\alpha_{13} z)+x_2x_3(\beta_{23}+\alpha_{23} z) \quad \text{(Eq. 1)}$$

Where, E(y) is the mean value of the response variable (shape parameters, textural and rheological parameters), x_i is the individual constituent of the mixture (1 = syrup, 2 = xanthan

gum, and 3 = KGM), $x_i x_j$ represent constituent interactions, z process variable (temperature), and β_i, β_{ij}, α_i, and α_{ij} are parameters.

3. Results and discussion

3.1. Rheological and viscoelastic behaviour

Figure 3 shows the elastic modulus (G'), viscous modulus (G"), apparent viscosity (η*), and tan δ, as a function of temperature. For Figure 3 the heating rate was 2 ºC/min for a syrup-xanthan gum–KGM (97.975, 0.575, 1.45) mixture. Table 2 shows the values of the rheological parameters for all the mixtures evaluated in this work at 20 ºC and 50 ºC. In Figure 3 the mixture shows a melting transition, with a sigmoidal reduction in apparent viscosity (η*), G', and G" moduli, with a sigmoidal increase in tan δ, this behaviour was detected in all mixtures analysed. These changes in moduli have been studied by other authors (Abbaszadeh, Macnaughtan, Sworn, & Foster, 2016; Fitzsimons, Tobin, & Morris, 2008). Abbaszadeh et al. (2016) proposed two types (A and B) of interaction in KGM/xanthan gels. In the type A interaction, xanthan keeps its helical conformation and the formed gel melts at a lower temperature range, approximately 30 ºC – 45 ºC. The type B interaction occurs with xanthan, through a disordered conformation where the formed gel melts at the higher temperature of approximately 60 ºC. The xanthan transition temperature is the key parameter in determining the type of interaction and can be manipulated by changing environmental conditions such as ionic concentration, pH, and functional group content (Abbaszadeh et al., 2016).

The mixtures studied in this work, present an interaction type A, with a melting temperature about 45 ºC. In this work the printing temperatures studied (25 ºC and 50 ºC) strongly affect the rheological characteristics of the gel, as implies a different interaction type. The values in Table 2 reflect this change. Values of G' of samples printed at 25 ºC, ranged between 1528 Pa and 1006 Pa while samples printed at 50 ºC showed G' values between 390 Pa and 644 Pa. Values of G" of samples printed at 25 ºC ranged between 340 Pa and 227 Pa while samples printed at

50 ºC showed G" values between 244 Pa and 153 Pa. Changes in elastic modulus (G') with temperature, were more relevant than changes in viscous modulus (G"). Samples printed at 50 ºC were less elastic that samples printed at 25 ºC. The values of viscosity (Table 2) also reflect the higher fluidity of samples printed at 50 ºC, with lower values of η*. Regarding the effect of composition on rheological properties, the higher values of G', G" and η* were obtained in the mixtures with lower syrup concentration but higher values of xanthan gum and KGM (Table 2).

When mixing KGM with xanthan gum, a thermo-reversible gel can be produced with a gel strength dependent on gum concentration, a higher gum concentration implies higher strength. In this work the ratio of KGM/xanthan gum ranged between 1.9 and 3.3. Mao et al. (2012) studied ratios of KGM/xanthan gum between 0.1 and 10 and reported that the elastic moduli (G') for samples of ratio near to 2, are consistently higher than those of different mixing ratios at all concentrations.

3.2. Extrusion behaviour

Typical force-versus-time curves obtained for different temperatures during forward extrusion measurements are shown in Figure 4. The curves reflect the different stages during extrusion. The piston was pushed onto the sample, compressing the sample to pack more tightly. In this stage, between 0 and 30 s, the force increased steeply, and the extrusion occurred. Once the force increased to a maximum point, a plateau was observed, at time 65 s. The plateau was considered as the force required to continue the extrusion. The slope of the curve during the ten first seconds (N/s), the maximum force (N) needed for move the piston10 mm, the mean force applied in the plateau (N) during 60 s, and the area under the curve force-time (N s) during 60 s were used to characterise the samples (Figure 4). Seen in Figure 4, curves of samples extruded at 50 ºC present a slope with a lesser gradient, lower maximum force, and a plateau with more uniformity than samples extruded at 25 ºC.

Table 2 shows the values of these parameters for all the mixtures evaluated in this work at 25 ºC and 50 ºC. Values of Fmax (N), Fmean (N), and area (N s) were greater for samples extruded at

25 ºC. The gradient values of extrusion curves were also greater (1.87 - 1.64 N/s) in samples extruded at 25 ºC than values of samples extruded at 50 ºC (1.62 - 1.38 N/s). The slope and Fmax values are related with the stiffness and firmness of the gels, respectively.

Conformational ordering, and associated development of xanthan ‘‘weak gel’’ structure, at a progressively higher temperature, explains the decrease in extrusion parameters value observed (Agoub, Smith, Giannouli, Richardson, & Morris, 2007). syrup, xanthan gum, and KGM content influences the textural properties. With the increase of syrup content, the Fmax, Fmean, area, and slope gradient were reduced giving more weak gels. This is mainly because of the reduction of the other components that implies a reduction in the number of synergic interactions between xanthan gum/KGM (Abbaszadeh et al., 2016).

3.3. 3D Printing

An ideal gel should have a well-defined network, sufficiently high gel strength, with proper viscosity, and be printable below the extrusion pressure of the printer and still capable of fusing with earlier printed layers, while keeping the print shape (Godoi et al., 2016). Figure 5 shows the effect of printing temperature on printing quality of 3D constructs. The same mixture composition using different temperatures, 50 ºC and 25 ºC, strongly affected the result. Temperatures of 50 ºC resulted in the relatively delicate but well-defined models. However, as shown in the Figure 5 gels printed at 25 ºC resulted in poor models. It should be mentioned that the use of a lower diameter nozzle could provide better defined models.

Table 1 shows the shape parameters (area and height) obtained from printed figures at 5 min and 1 h after printing. The height of the printed figure (star) was designed to be 2 cm. As seen in Table 1, figures printed at 50 ºC almost achieve this height, while figures printed at 25 ºC result in lower constructs. However, a trend of reduced height with time was observed in all samples. This trend is related with the viscoelastic characteristics of the gels. In this study, an expansion occurs sometimes (reduction in height and an increase in area) after 1 h.

Shape parameters were fitted to a model that include components of the mixture and their interactions and temperature of printing (equation 1). Table 3 shows the parameters of the model and coefficients of determination (R^2). As can be observed in Table 3 the most important effect is the additive effect of each component of the mixture (β_i parameters). The nonlinear synergistic binary effect (β_{ij} parameters) are not significant. With respect to process variables the effect on temperature on xanthan gum (α_2) is very significant in the height of the figure (H 5 min and H 1 h).

Figure 6 shows the optimisation plot obtained by Minitab. The optimisation plot shows the effect of each factor (columns) on the responses or composite desirability (rows). The vertical red lines on the graph represent the current factor settings. The numbers displayed at the top of a column show the current factor level settings (in red) and the high and low value showed in each graphic (black). The first column shows the variables optimized with their target. The horizontal blue lines and numbers represent the responses for the current factor level. An optimisation plot is a response optimiser tool that shows how different experimental settings affect the predicted responses for a stored model. Minitab calculates an optimal solution and draws the plot.

Here, the goal used for the optimisation was to maximise the height of the figure after 5 min and 1 h while maintaining the area of the figure near 12.3 cm^2. These parameters relate to the maintenances of the figure form. A decrease in height and an increase in area implies a less stable figure. The optimal composition obtained for the three-component mixture (food-ink) was: syrup, 0.9773; xanthan gum, 0.0062; KGM, 0.0165 with 50 ºC as a process variables (temperature of printing) for the printing of a five points star.

3.4. Correlation between rheological/textural properties and printing

Another approach studied was to correlate rheological and textural parameters with printing parameters. Then knowing the values of these parameters, predicting the printability of the figure would be possible. For this purpose, rheological and textural parameters were fitted to

equation 1. Table 4 shows the parameters and coefficients of determination (R^2) obtained. As can be observed in Table 4 the most important effect for rheological and textural parameters is the additive effect of each component of the mixture (β_i parameters). In the case of the rheological parameters the effect of temperature on each component of the mixture (α_i parameters) is very significant. With respect to the nonlinear synergistic binary effect (β_{ij} parameters) only the interaction between syrup and xanthan gum is significant for G´, tan δ, and η*. For textural parameters (Fmax, Fmean, and Area) is the effect of temperature on the interaction xanthan gum with KGM (α_{23} parameter) the effect most significant. From the fitted models, contour plots provided by Minitab were used to analyse relationships between shape parameters and rheological and textural parameters.

A contour plot displays a two-dimensional view, where points that have the same response value, are connected to produce contour lines. Figure 7 represent the contour plot corresponding to shape parameters of the figure (height and area). As observed in Figure 7, the lesser interception area corresponds to the height and area of the figure after 1 hour. This means that samples maintain a height, up to 1.7 cm and an area lower than 12.5 cm^2 after 1 h; also sample have a height up to 1.8 cm after 5 min with an area between 11.5 and 12.5 cm^2. Therefore, the critical (most restrictive) parameter in this case is the height and area of the figure after 1 hour.

Figure 8 shows the contour plots corresponding to the rheological parameters (Figure 8a) and textural parameters (Figure 8b) that best fit to the most restrictive shape parameters (height up to 1.7 cm and area lower than 12.5 cm^2 after 1 hour). As seen in Figure 8a the area defined by tan δ between 0.365 and 0.38, viscosity between 102 Pa s and 113 Pa s, and G' between 595 Pa and 660 Pa fit properly with the area defined by the critical parameters. With of textural parameters (Figure 8b), the best fit with the most restrictive form parameters is achieved by the area defined by Fmax between 60 N and 68 N and slope gradient between 1.47 N/s and 1.49 N/s.

Comparing Figures 8a and 8b, both rheological and textural parameters can provide a good fit with shape parameters. Comparing Tables 2 and 4, samples with values of rheological parameters near to values mentioned before, provided good 3D printed figures. These rheological and textural values correspond to formulas with a composition similar to the optimal variation, described previously.

In conclusion, it is possible, from the study of rheological properties of gels to establish values of key parameters that can help to ensure printability of figures under controlled process conditions. If values of these parameters can be defined, it will be easier to develop 3D printing products at home, for regular consumers.

4. Conclusions

In this investigation the printing temperatures studied (25 ºC and 50 ºC) strongly affect rheological characteristics of the gel as implies a different interaction type. Samples printed at 50 ºC were less elastic and had greater fluidity than samples printed at 25 ºC. Regarding the effect of composition on rheological properties; higher values of G', G", and η* were obtained in the mixtures with lower syrup concentration, and with greater content of xanthan gum and KGM. The textural properties were influenced by syrup, xanthan gum, and KGM content. With the increase of syrup content, the Fmax, Fmean, area, and slope gradient were reduced. This is due to the reduction of the other mixture components, implying a reduction in the number of synergic interactions between xanthan gum and KGM. In conclusion, this study shows that rheological and textural values can define composition of formulations that give rise to valid 3D printed figures. This kind of information can help to develop in the future an automatic configuration in 3D printers without intervention of the final user. From textural or rheological properties of foods, optimal printing conditions will be defined helping people in the use of this technology.

Funding sources

This research did not receive any specific grant from funding agencies in the public, commercial, or not-for-profit sectors.

References

Abbaszadeh, A., Macnaughtan, W., Sworn, G., & Foster, T. J. (2016). New insights into xanthan synergistic interactions with konjac glucomannan: A novel interaction mechanism proposal. *Carbohydrate Polymers*, *144*, 168–177. https://doi.org/10.1016/j.carbpol.2016.02.026

Abramoff, M. D., Magalhães, P. J., & Ram, S. J. (2004). Biophotonics international. *Biophotonics International*, *11*(7), 36–42. Retrieved from https://dspace.library.uu.nl/handle/1874/204900

Agoub, A. A., Smith, A. M., Giannouli, P., Richardson, R. K., & Morris, E. R. (2007). "Melt-in-the-mouth" gels from mixtures of xanthan and konjac glucomannan under acidic conditions: A rheological and calorimetric study of the mechanism of synergistic gelation. *Carbohydrate Polymers*, *69*(4), 713–724. https://doi.org/10.1016/j.carbpol.2007.02.014

Cornell, J. A. (1990). *Experiments with mixtures : designs, models and the analysis of mixture data* (2nd ed.). New York: John Wiley & Sons.

Derossi, A., Caporizzi, R., Azzollini, D., & Severini, C. (2018). Application of 3D printing for customized food. A case on the development of a fruit-based snack for children. *Journal of Food Engineering*, *220*, 65–75. https://doi.org/10.1016/j.jfoodeng.2017.05.015

Diañez, I., Gallegos, C., Brito-de la Fuente, E., Martínez, I., Valencia, C., Sánchez, M. C., … Franco, J. M. (2019). 3D printing in situ gelification of κ-carrageenan solutions: Effect of printing variables on the rheological response. *Food Hydrocolloids*, *87*(July 2018), 321–330. https://doi.org/10.1016/j.foodhyd.2018.08.010

Fitzsimons, S. M., Tobin, J. T., & Morris, E. R. (2008). Synergistic binding of konjac glucomannan to xanthan on mixing at room temperature. *Food Hydrocolloids*, *22*(1), 36–46. https://doi.org/10.1016/j.foodhyd.2007.01.023

Godoi, F. C., Prakash, S., & Bhandari, B. R. (2016). 3d printing technologies applied for food

design: Status and prospects. *Journal of Food Engineering*. https://doi.org/10.1016/j.jfoodeng.2016.01.025

Hamilton, C. A., Alici, G., & in het Panhuis, M. (2018). 3D printing Vegemite and Marmite: Redefining "breadboards." *Journal of Food Engineering*, *220*, 83–88. https://doi.org/10.1016/j.jfoodeng.2017.01.008

Holland, S., Foster, T., MacNaughtan, W., & Tuck, C. (2018). Design and characterisation of food grade powders and inks for microstructure control using 3D printing. *Journal of Food Engineering*, *220*, 12–19. https://doi.org/10.1016/j.jfoodeng.2017.06.008

Le Tohic, C., O'Sullivan, J. J., Drapala, K. P., Chartrin, V., Chan, T., Morrison, A. P., … Kelly, A. L. (2018). Effect of 3D printing on the structure and textural properties of processed cheese. *Journal of Food Engineering*, *220*, 56–64. https://doi.org/10.1016/j.jfoodeng.2017.02.003

Lipson, H., & Kurman, M. (2013). *Fabricated: The New World of 3D PrintingNo Title*. New York: John Wiley and Sons, Inc.

Liu, Z., Bhandari, B., Prakash, S., Mantihal, S., & Zhang, M. (2019). Linking rheology and printability of a multicomponent gel system of carrageenan-xanthan-starch in extrusion based additive manufacturing. *Food Hydrocolloids*, *87*(August 2018), 413–424. https://doi.org/10.1016/j.foodhyd.2018.08.026

Liu, Z., Zhang, M., Bhandari, B., & Wang, Y. (2017, September). 3D printing: Printing precision and application in food sector. *Trends in Food Science and Technology*. https://doi.org/10.1016/j.tifs.2017.08.018

Liu, Z., Zhang, M., Bhandari, B., & Yang, C. (2018). Impact of rheological properties of mashed potatoes on 3D printing. *Journal of Food Engineering*, *220*, 76–82. https://doi.org/10.1016/j.jfoodeng.2017.04.017

Mao, C. F., Klinthong, W., Zeng, Y. C., & Chen, C. H. (2012). On the interaction between

konjac glucomannan and xanthan in mixed gels: An analysis based on the cascade model. *Carbohydrate Polymers*, *89*(1), 98–103. https://doi.org/10.1016/j.carbpol.2012.02.056

Severini, C., Azzollini, D., Albenzio, M., & Derossi, A. (2018). On printability, quality and nutritional properties of 3D printed cereal based snacks enriched with edible insects. *Food Research International*, *106*(January), 666–676. https://doi.org/10.1016/j.foodres.2018.01.034

Severini, Carla, & Derossi, A. (2016). Could the 3D Printing Technology be a Useful Strategy to Obtain Customized Nutrition? *Journal of Clinical Gastroenterology*, *50*, S175–S178. https://doi.org/10.1097/MCG.0000000000000705

Sun, J., Peng, Z., Zhou, W., Fuh, J. Y. H., Hong, G. S., & Chiu, A. (2015). A Review on 3D Printing for Customized Food Fabrication. *Procedia Manufacturing*, *1*, 308–319. https://doi.org/10.1016/j.promfg.2015.09.057

Wang, L., Zhang, M., Bhandari, B., & Yang, C. (2018). Investigation on fish surimi gel as promising food material for 3D printing. *Journal of Food Engineering*, *220*, 101–108. https://doi.org/10.1016/j.jfoodeng.2017.02.029

Yang, Fan, Zhang, M., & Bhandari, B. (2017). Recent development in 3D food printing. *Critical Reviews in Food Science and Nutrition*, *57*(14), 3145–3153. https://doi.org/10.1080/10408398.2015.1094732

Yang, Fanli, Zhang, M., Bhandari, B., & Liu, Y. (2018). Investigation on lemon juice gel as food material for 3D printing and optimization of printing parameters. *LWT - Food Science and Technology*, *87*, 67–76. https://doi.org/10.1016/j.lwt.2017.08.054

Zhang, M., Vora, A., Han, W., Wojtecki, R. J., Maune, H., Le, A. B. A., … Nelson, A. (2015). Dual-Responsive Hydrogels for Direct-Write 3D Printing. *Macromolecules*, *48*(18), 6482–6488. https://doi.org/10.1021/acs.macromol.5b01550

Figure captions

Figure 1. a) Dimensions of printed figure b) 3D printer BCN 3D+ with cooling system.

Figure 2. Shape parameters measured in the printed figure. A, area (cm^2); H_1 and H_2, height (cm).

Figure 3. Elastic modulus (G'), viscous modulus (G"), apparent viscosity (η*), and tan δ, as a function of temperature with a heating rate of 2 ºC/min for a syrup-xanthan gum–KGM (97.975, 0.575, 1.45) mixture.

Figure 4. Example of force-versus-time curves during forward extrusion measurement for a syrup-xanthan gum–KGM mixture at different temperatures, 25 ºC and 50 ºC.

Figure 5. Example of 3D printed gels after 5 min and 1 h of printing. a) syrup-xanthan gum–KGM: 0.97975, 0.00575, 0.0145 at 50 ºC; b) syrup-xanthan gum–KGM: 0.978375, 0.006125, 0.0155 at 25 ºC; c) syrup-xanthan gum–KGM: 26 0.97975, 0.00575, 0.0145 at 25 ºC.

Figure 6. Optimisation plot showing how different experimental settings (components of the mixture and temperature) affect the predicted responses for a stored model. A 5 min, area of the star after five minutes of printing (cm^2); A 1 h, area of the star after one hour of printing (cm^2); H 5 min, height of the star after five minutes of printing (cm); H 1 h, height of the star after one hour of printing (cm).

Figure 7. Contour plot corresponding to shape parameters of the figure (height and area). A contour plot displays a two-dimensional view in which points that have the same response value are connected to produce contour lines.

Figure 8. Contour plots corresponding to the rheological parameters (a) and textural parameters (b), that best fit with the most restrictive shape parameters. A contour plot displays a two-dimensional view in which points that have the same response value are connected to produce contour lines.

Table 1. Mixing design and shape parameters of printed figures with different mixtures at 25 ºC and 50 ºC. A 5 min, area of the star after five minutes of printing (cm^2); A 1 h, area of the star after one hour of printing (cm^2); H 5 min, height of the star after five minutes of printing (cm); H 1 h, height of the star after one hour of printing (cm).

StdOrder (SO)	Syrup	Xanthan Gum	KGM	T (ºC)	A 5 min (cm^2)	A 1 h (cm^2)	H 5 min (cm)	H 1 h (cm)
1	0.9785	0.005	0.0165	25	11.3 ± 0.9	10.6 ± 1.0	1.38 ± 0.11	1.15 ± 0.08
2	0.977	0.0065	0.0165	25	10.3 ± 0.6	11.3 ± 0.5	1.51 ± 0.04	1.35 ± 0.00
3	0.9825	0.005	0.0125	25	12.6 ± 0.5	14.2 ± 0.5	1.86 ± 0.04	1.64 ± 0.17
4	0.981	0.0065	0.0125	25	9.2 ± 1.2	9.0 ± 1.1	0.64 ± 0.07	0.58 ± 0.06
5	0.9805	0.005	0.0145	25	12.3 ± 0.4	13.5 ± 0.4	1.94 ± 0.04	1.60 ± 0.07
6	0.98175	0.00575	0.0125	25	7.8 ± 1.3	7.7 ± 1.2	0.58 ± 0.11	0.52 ± 0.13
7	0.979	0.0065	0.0145	25	8.8 ± 1.3	7.7 ± 1.1	0.32 ± 0.05	0.33 ± 0.01
8	0.97775	0.00575	0.0165	25	10.6 ± 1.1	11.1 ± 1.2	0.63 ± 0.01	0.61 ± 0.02
9	0.97975	0.00575	0.0145	25	10.4 ± 0.8	10.2 ± 0.9	0.96 ± 0.04	0.90 ± 0.04
10	0.979125	0.005375	0.0155	25	9.2 ± 1.4	9.7 ± 1.2	0.70 ± 0.02	0.62 ± 0.03
11	0.978375	0.006125	0.0155	25	10.9 ± 1.1	10.6 ± 1.3	1.03 ± 0.02	0.99 ± 0.02
12	0.981125	0.005375	0.0135	25	11.3 ± 0.5	11.8 ± 0.6	1.98 ± 0.09	1.76 ± 0.09
13	0.980375	0.006125	0.0135	25	12.9 ± 0.4	13.5 ± 0.3	1.96 ± 0.06	1.77 ± 0.11
14	0.9785	0.005	0.0165	50	12.7 ± 0.4	13.5 ± 0.4	1.91 ± 0.00	1.59 ± 0.07
15	0.977	0.0065	0.0165	50	11.7 ± 0.5	12.0 ± 0.6	1.79 ± 0.04	1.61 ± 0.01
16	0.9825	0.005	0.0125	50	13.2 ± 0.2	14.5 ± 0.3	1.87 ± 0.04	1.54 ± 0.08
17	0.981	0.0065	0.0125	50	12.7 ± 0.3	13.4 ± 0.4	1.89 ± 0.00	1.58 ± 0.05
18	0.9805	0.005	0.0145	50	12.2 ± 0.3	15.2 ± 0.2	1.93 ± 0.04	1.62 ± 0.03
19	0.98175	0.00575	0.0125	50	12.5 ± 0.3	14.4 ± 0.3	1.97 ± 0.08	1.71 ± 0.07
20	0.979	0.0065	0.0145	50	10.7 ± 0.6	10.8 ± 0.7	1.90 ± 0.04	1.72 ± 0.07
21	0.97775	0.00575	0.0165	50	12.2 ± 0.3	12.6 ± 0.3	1.94 ± 0.04	1.75 ± 0.10
22	0.97975	0.00575	0.0145	50	12.3 ± 0.4	12.0 ± 0.5	1.96 ± 0.03	1.82 ± 0.01
23	0.979125	0.005375	0.0155	50	12.2 ± 0.3	14.1 ± 0.3	1.92 ± 0.07	1.52 ± 0.15
24	0.978375	0.006125	0.0155	50	12.3 ± 0.4	12.9 ± 0.3	2.03 ± 0.04	1.83 ± 0.04
25	0.981125	0.005375	0.0135	50	12.4 ± 0.4	14.3 ± 0.5	1.88 ± 0.02	1.62 ± 0.01
26	0.980375	0.006125	0.0135	50	11.6 ± 0.4	11.8 ± 0.4	1.89 ± 0.07	1.68 ± 0.16

Table 2. Rheological parameters from oscillation test and parameters from the compression force-time curves of different mixtures at 25 ºC and 50 ºC. G', elastic modulus (Pa); G'', viscous modulus (Pa); tan δ; η*, apparent viscosity (Pa s); Slope, slope of the curve in the first 10 s of the test (N/s); Fmax, maximum force achieved (N); Fmean, mean value of the plateau force (N); Area, area defined under the curve in the plateau zone (N s).

Std Order (SO)	G' (Pa)	G" (Pa)	tan δ	η* (Pa s)	Slope (N/s)	Fmax (N)	Fmean (N)	Area (N s)
1	1265 ± 76	316 ± 10	0.250 ± 0.008	208 ± 12	1.84 ± 0.08	76 ± 5	73 ± 4	4398 ± 248
2	1528 ± 48	337 ± 8	0.220 ± 0.003	249 ± 8	1.75 ± 0.05	93 ± 10	82 ± 4	4901 ± 236
3	1071 ± 63	238 ± 10	0.223 ± 0.006	175 ± 10	1.84 ± 0.13	54 ± 2	47 ± 1	2837 ± 71
4	1149 ± 38	251 ± 6	0.218 ± 0.005	187 ± 6	1.79 ± 0.12	48 ± 5	41 ± 2	2433 ± 108
5	1212 ± 81	275 ± 9	0.228 ± 0.010	198 ± 13	1.74 ± 0.04	49 ± 7	46 ± 5	2750 ± 286
6	1006 ± 22	227 ± 4	0.226 ± 0.001	164 ± 4	1.72 ± 0.07	56 ± 5	47 ± 1	2801 ± 46
7	1282 ± 75	278 ± 8	0.217 ± 0.007	209 ± 12	1.64 ± 0.08	81 ± 3	72 ± 1	4331 ± 58
8	1447 ± 78	340 ± 17	0.235 ± 0.002	237 ± 13	1.65 ± 0.03	85 ± 4	83 ± 5	4951 ± 291
9	1234 ± 134	285 ± 20	0.232 ± 0.008	202 ± 21	1.71 ± 0.08	65 ± 4	60 ± 3	3621 ± 184
10	1181 ± 16	266 ± 2	0.225 ± 0.003	193 ± 2	1.78 ± 0.02	51 ± 4	48 ± 4	2882 ± 236
11	1461 ± 128	326 ± 20	0.224 ± 0.006	238 ± 21	1.87 ± 0.11	70 ± 8	61 ± 6	3680 ± 341
12	1106 ± 90	264 ± 17	0.239 ± 0.006	181 ± 15	1.79 ± 0.10	47 ± 1	42 ± 2	2514 ± 91
13	12 ± 91	27 ± 17	0.21 ± 0.00	20 ± 15	1.8 ± 0.02	58 ± 1	55 ± 2	3298 ± 10

	59			0			4		5	5			7												7
14	584	±	21	233	±	7	0.399	±	0.004	100	±	4	1.50	±	0.06	80	±	3	79	±	2	4723	±	13	2
15	644	±	17	236	±	6	0.367	±	0.002	109	±	3	1.43	±	0.02	65	±	1	63	±	1	3778	±	47	
16	413	±	22	164	±	6	0.398	±	0.007	71	±	4	1.54	±	0.02	49	±	6	48	±	5	2879	±	30	5
17	453	±	9	168	±	2	0.370	±	0.007	77	±	1	1.45	±	0.06	40	±	2	39	±	2	2331	±	14	9
18	477	±	27	193	±	8	0.404	±	0.009	82	±	4	1.49	±	0.01	43	±	5	42	±	6	2550	±	35	0
19	390	±	10	153	±	3	0.391	±	0.003	67	±	2	1.44	±	0.02	44	±	1	43	±	1	2587	±	51	
20	521	±	30	193	±	8	0.371	±	0.007	88	±	5	1.50	±	0.11	67	±	2	66	±	2	3953	±	92	
21	627	±	32	244	±	11	0.390	±	0.002	107	±	5	1.62	±	0.03	65	±	3	63	±	3	3781	±	19	9
22	508	±	65	200	±	18	0.395	±	0.014	87	±	11	1.47	±	0.04	56	±	3	55	±	3	3301	±	16	3
23	486	±	11	193	±	3	0.397	±	0.004	83	±	2	1.55	±	0.06	40	±	2	39	±	2	2357	±	11	2
24	608	±	53	228	±	14	0.376	±	0.010	103	±	9	1.42	±	0.05	44	±	4	43	±	3	2566	±	18	8
25	452	±	36	183	±	12	0.404	±	0.009	78	±	6	1.41	±	0.04	45	±	2	44	±	2	2662	±	12	8
26	493	±	26	186	±	9	0.378	±	0.003	84	±	4	1.38	±	0.06	54	±	1	52	±	1	3125	±	87	

Table 3. Parameters of mixture-process variable design and determination coefficient (R^2) for the model fitted to predict the response variables (shape parameters) as a function of the independent variables (composition and process temperature). A 5 min, area of the star after five minutes of printing (cm^2); A 1 h, area of the star after one hour of printing (cm^2); H 5 min, height of the star after five minutes of printing (cm); H 1 h, height of the star after one hour of printing (cm).

	A 5 min (cm^2)	H 5 min (cm)	A 1 h (cm^2)	H 1 h (cm)
β_1	12.157	1.983	14.404	1.693
β_2	7.19	1.83	10.11	2.02
β_3	11.939	1.393	11.69	1.169
β_{12}	-	-3.37^{ns}	-14.00^{ns}	-3.18^{ns}
β_{13}	-	-	-	-
β_{23}	-	-	-	-
α_1	-	-	0.915^{ns}	-
α_2	-	1.810^{**}	-	1.541^{**}
α_3	0.867^{*}	-	1.030^{ns}	-
α_{12}	7.65^{**}	-	6.38^{ns}	-
α_{13}	-	0.923^{ns}	-	0.748^{ns}
α_{23}	-	-	-	-
R^2(%)	50.26	59.00	63.27	56.02

Asterisks *, and** denote coefficients that are statistically significant with 90%, and 95% confidence, respectively. An ''ns'' denotes coefficients that are not statistically significant with at least 90% confidence. It is inappropriate to consider the statistical significance of the three linear mixture terms (Cornell, 2002)

Table 4. Parameters of the mixture-process variable design and determination coefficient (R^2) for the model fitted to predict the rheological and textural parameters as a function of the independent variables (composition and process temperature). G', elastic modulus (Pa); G'', viscous modulus (Pa); tan δ; η*, apparent viscosity (Pa s); Slope, slope of the curve in the first 10 s of the test (N/s); Fmax, maximum force achieved (N); Fmean, mean value of the plateau force (N); Area, area defined under the curve in the plateau zone (N s).

	G' (Pa)	G'' (Pa)	tan δ	η* (Pa s)	Slope (N/s)	Fmax (N)	Fmean (N)	Area (N s)
β_1	723.0	193.41	0.3131	119.58	1.6436	47.60	43.87	2633
β_2	1392	243.4	0.057	225.2	1.442	62.0	52.4	3145
β_3	998.8	303.56	0.3256	166.26	1.6628	88.35	84.28	5057
β_{12}	-607^{*}	-	0.251^{*}	-95.8^{*}	-	-	-	-
β_{13}	-	-	-	-	-	-51.4^{*}	-41.7^{ns}	-2504^{ns}
β_{23}	-	-	0.200^{ns}	-	-	-	-	-
α_1	-324.6^{***}	-35.62^{***}	0.0877^{***}	-51.23^{***}	-0.1647^{***}	-	-	-
α_2	-384^{**}	-57.7^{**}	0.0567^{***}	-61.5^{**}	-0.205^{ns}	-	-	-
α_3	-362.3^{***}	-45.7^{***}	0.0789^{***}	-57.10^{***}	-0.1000^{**}	-	-	-
α_{12}	-	-	-	-	-	-	-	-
α_{13}	-	-	-	-	-	-	-	-
α_{23}	-416^{ns}	-	-	-65.5^{ns}	-	-84.8^{***}	-58.6^{**}	-3518^{**}
R^2 (%)	98.97	95.87	99.66	98.90	84.75	68.82	65.23	65.23

Asterisks *, **, and *** denote coefficients that are statistically significant with 90%, 95%, and 99% confidence, respectively. An ''ns'' denotes coefficients that are not statistically significant with at least 90% confidence. It is inappropriate to consider the statistical significance of the three linear mixture terms (Cornell, 2002)

Conflicts of Interest

The authors confirm that there are no known conflicts of interest associated with this publication and there has been no significant financial support for this work that could have influenced its outcome.

Declaration of authors' contributions

V. García-Alcaraz: Methodology, Visualization, Formal analysis

S. Balasch-Parisi: Formal analysis, Methodology, Visualization.

Purificación García-Segovia: Conceptualization, Supervision, Writing - Review & Editing.

Javier Martínez-Monzó: Conceptualization, Methodology, Formal analysis, Supervision, Writing - Original Draft, Writing - Review & Editing.

Highlights

- Printability of syrup, xanthan, and konjac gels is affected by temperature.
- Gels printed at 50 ºC were less elastic and had greater fluidity.
- Higher G', G", and η* were obtained with greater content of xanthan gum and KGM
- Mixture design can help in 3D food printing modelling.

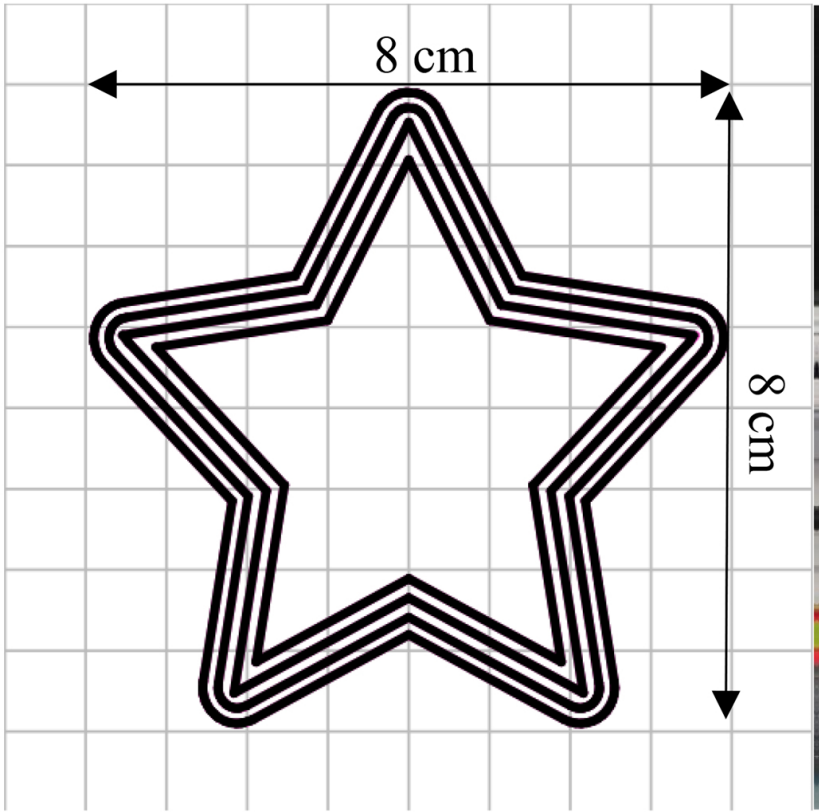

a

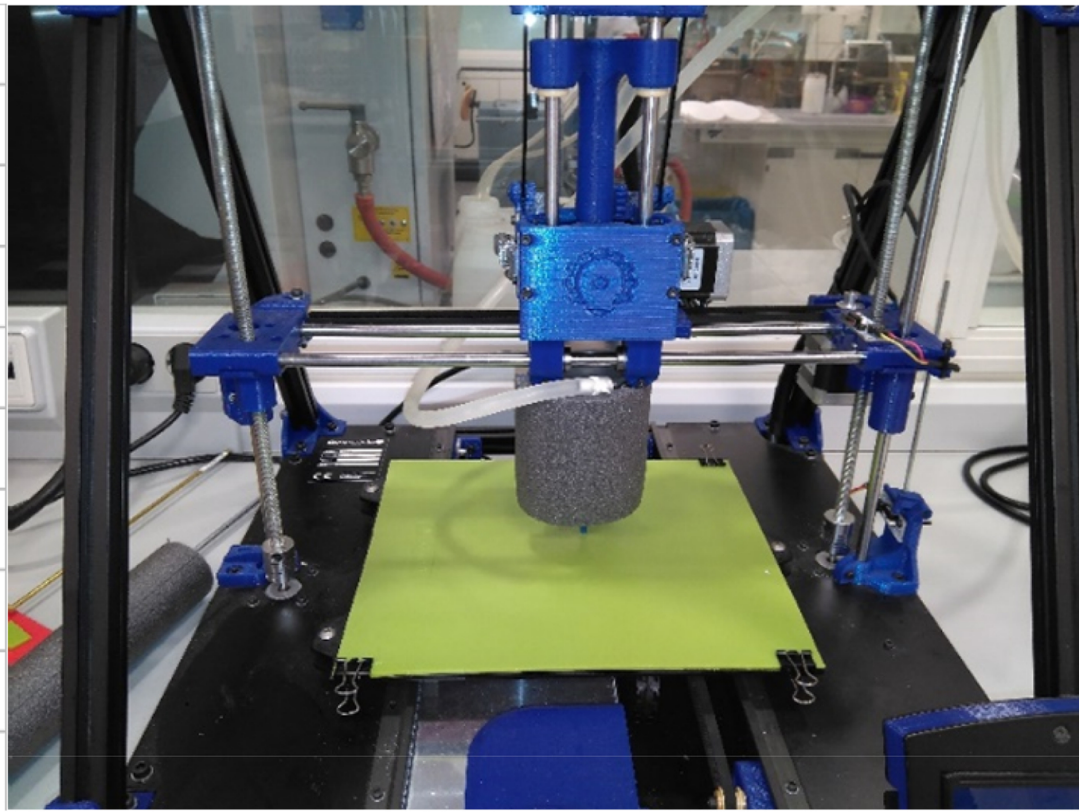

b

Figure 1

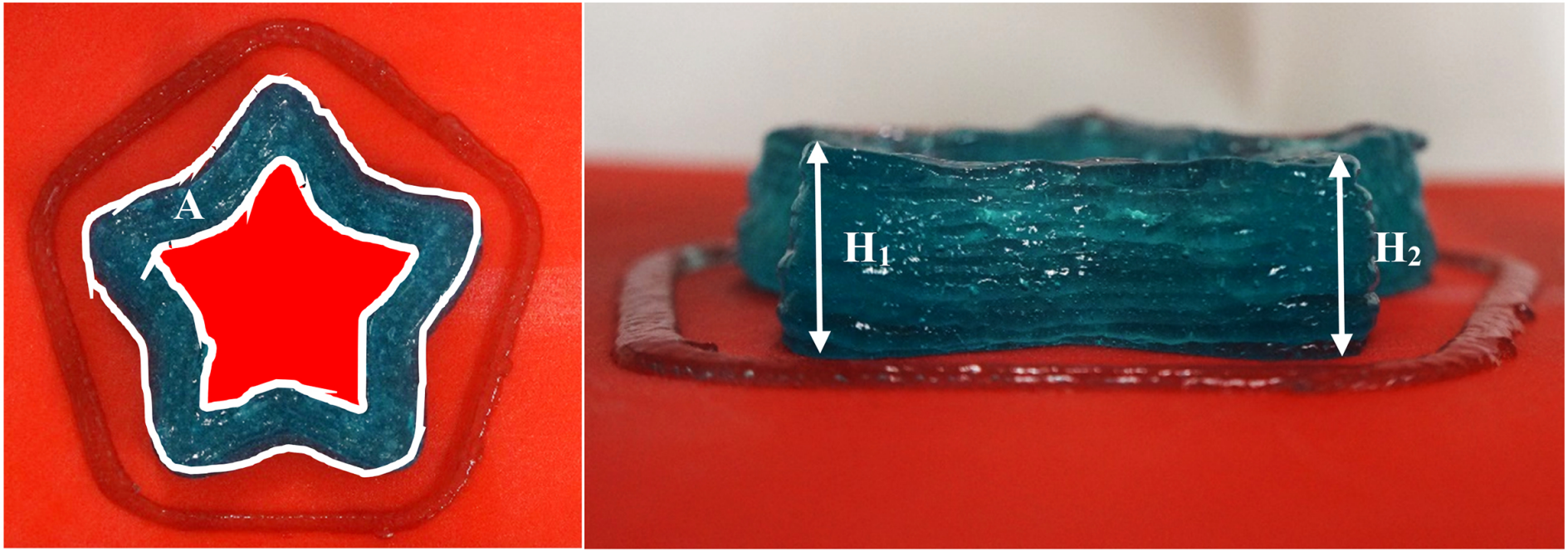

Figure 2

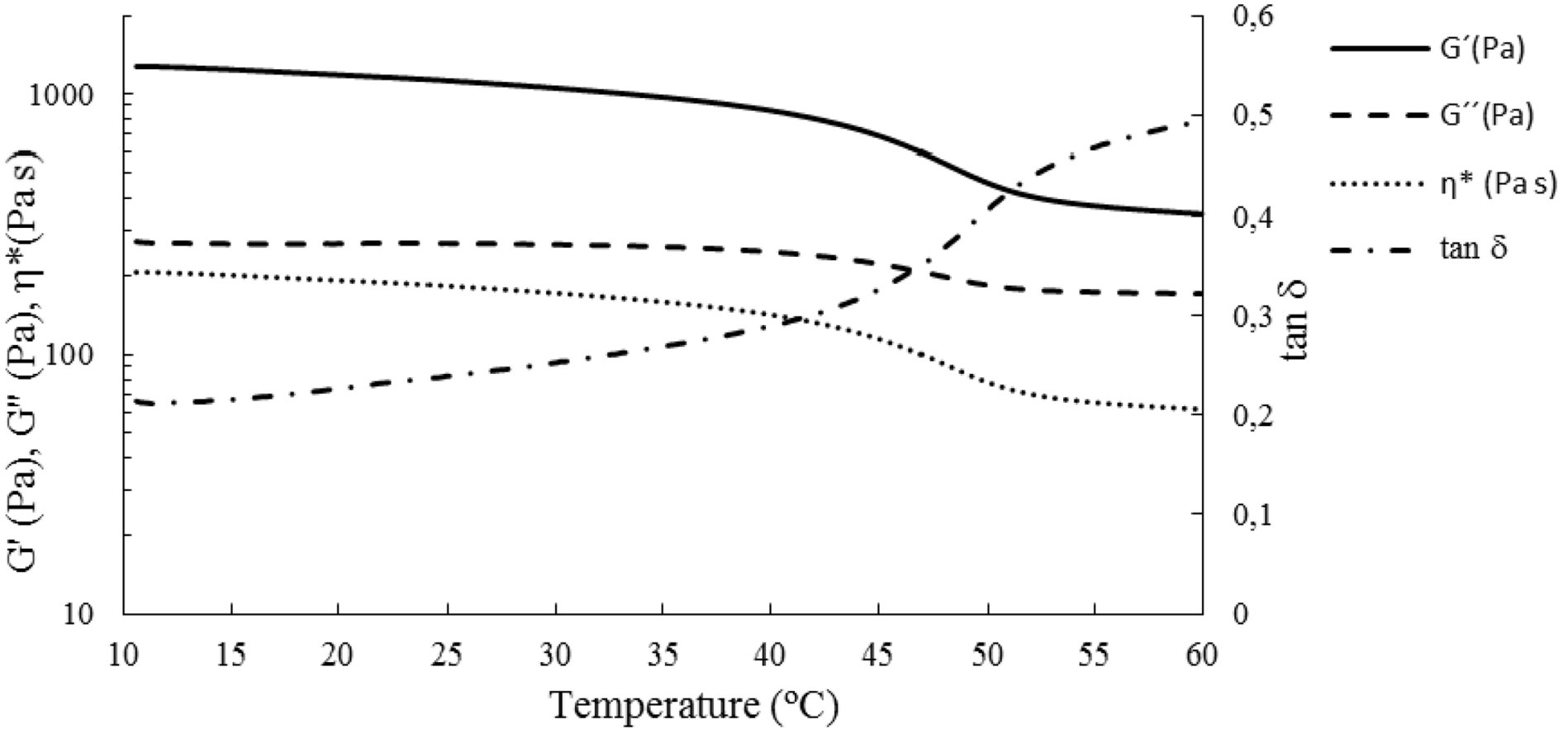
G' (Pa), G'' (Pa), η*(Pa s)
1000
100
10
10
15
20
25
30
35
40
45
50
55
60
Temperature (°C)
0,6
0,5
0,4
0,3
0,2
0,1
0
tan δ
G´(Pa)
G´´(Pa)
η* (Pa s)
tan δ

Figure 3

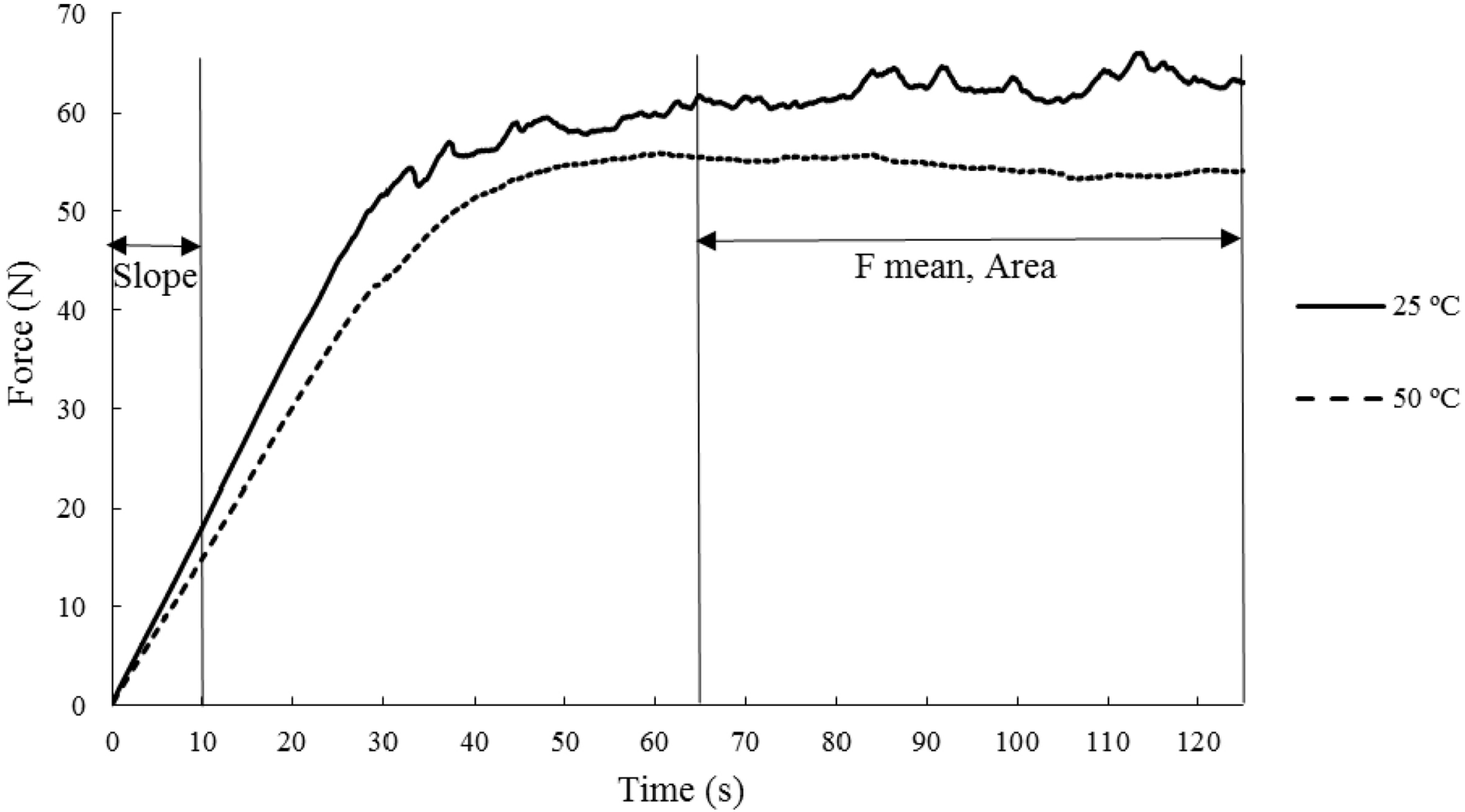
70
60
50
40
30
20
10
0
Force (N)
Slope
F mean, Area
0
10
20
30
40
50
60
70
80
90
100
110
120
Time (s)
25 °C
50 °C

Figure 4

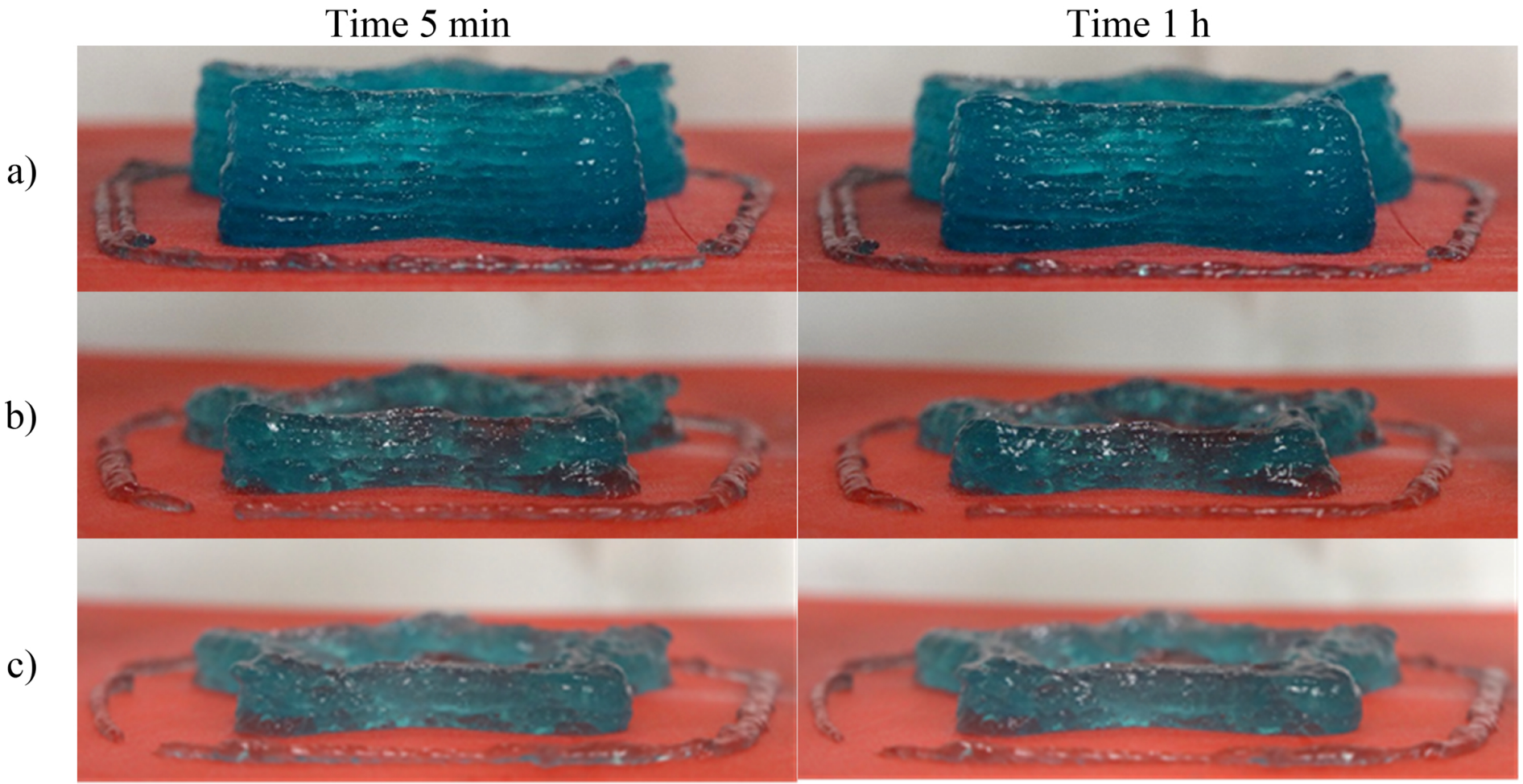

Figure 5

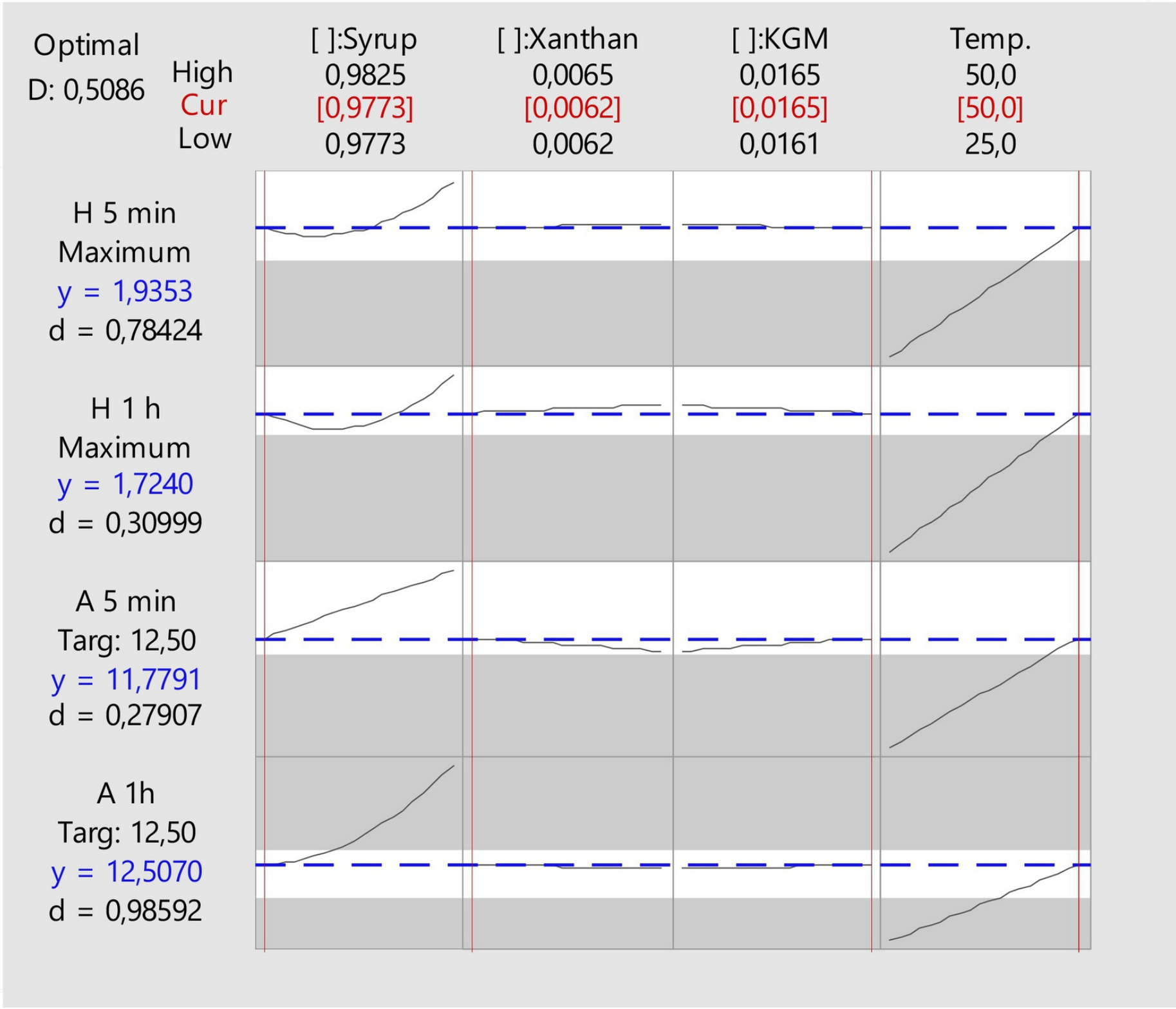
Optimal
D: 0,5086
High
Cur
Low
[ ]:Syrup
0,9825
[0,9773]
0,9773
[ ]:Xanthan
0,0065
[0,0062]
0,0062
[ ]:KGM
0,0165
[0,0165]
0,0161
Temp.
50,0
[50,0]
25,0
H 5 min
Maximum
y = 1,9353
d = 0,78424
H 1 h
Maximum
y = 1,7240
d = 0,30999
A 5 min
Targ: 12,50
y = 11,7791
d = 0,27907
A 1h
Targ: 12,50
y = 12,5070
d = 0,98592

Figure 6

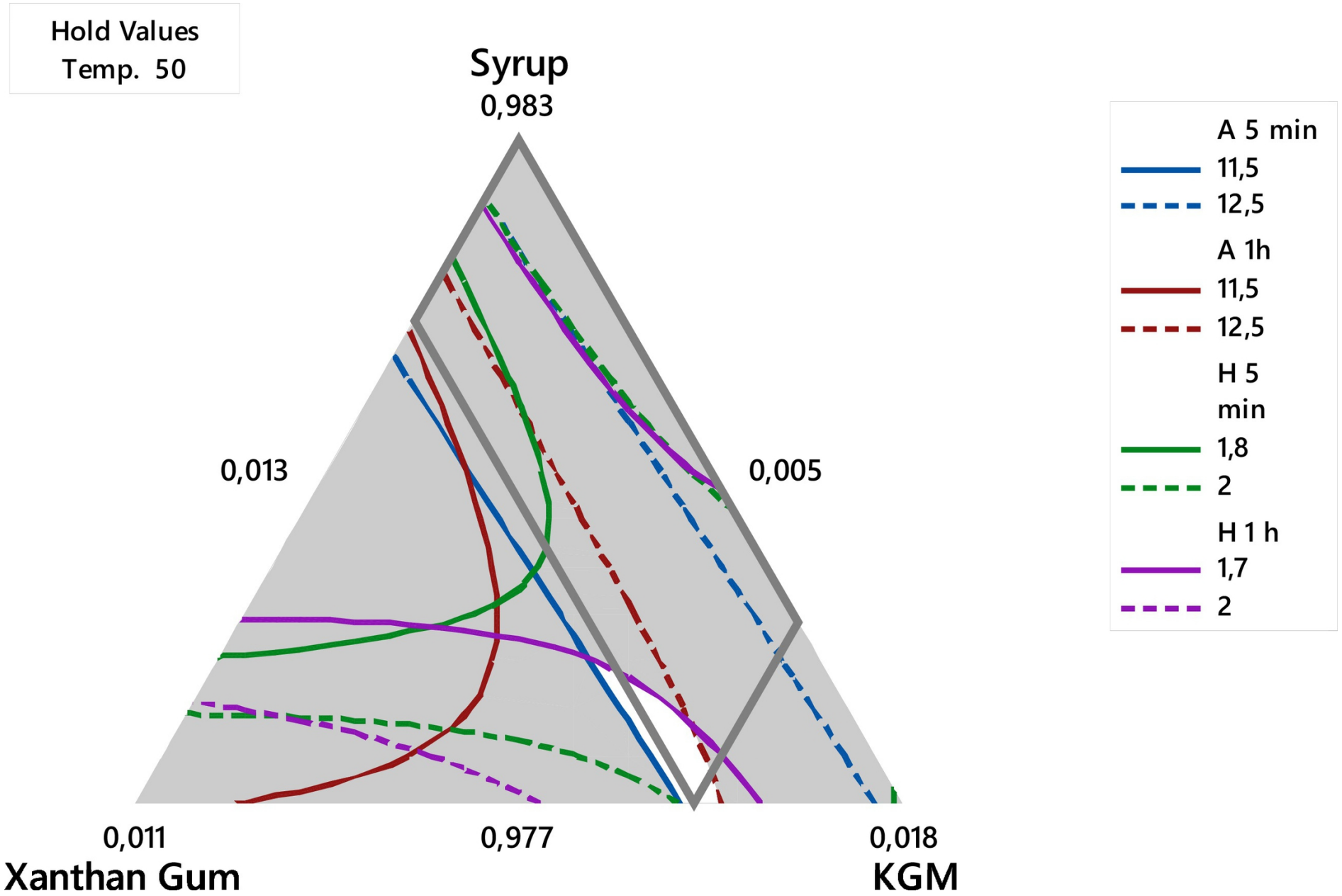
Hold Values
Temp. 50
Syrup
0,983
0,013
0,005
0,011
0,977
0,018
Xanthan Gum
KGM
A 5 min
11,5
12,5
A 1h
11,5
12,5
H 5 min
1,8
2
H 1 h
1,7
2

Figure 7

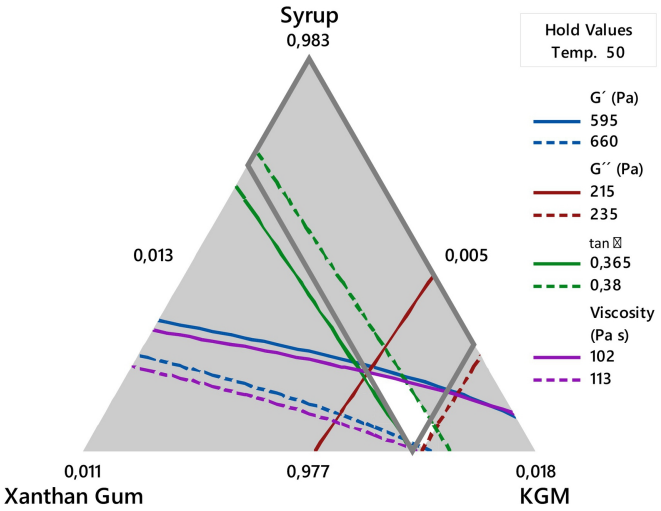
Syrup
0,983
0,013
0,005
0,011
0,977
0,018
Xanthan Gum
KGM
Hold Values
Temp. 50
G´ (Pa)
595
660
G´´ (Pa)
215
235
tan
0,365
0,38
Viscosity
(Pa s)
102
113

a)

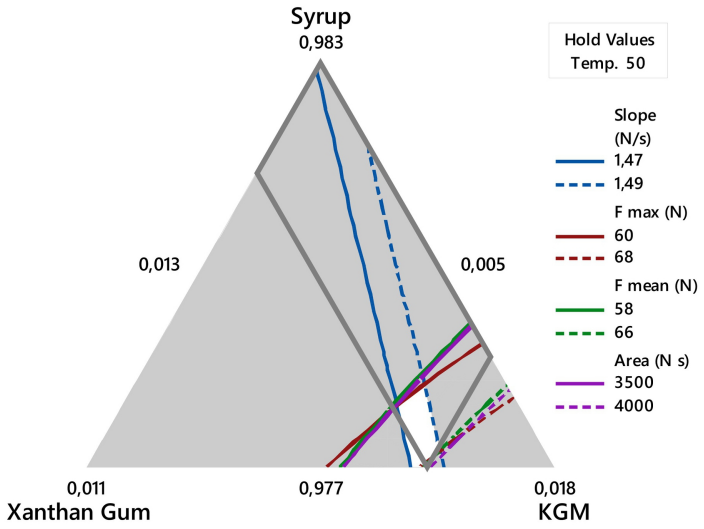
Syrup
0,983
0,013
0,005
0,011
0,977
0,018
Xanthan Gum
KGM
Hold Values
Temp. 50
Slope
(N/s)
1,47
1,49
F max (N)
60
68
F mean (N)
58
66
Area (N s)
3500
4000

b)

Figure 8